# Cellular concrete waste: An efficient new way for H2S removal

Morgane Poser, Luis Rodolfo Duarte E Silva, Pascal Peu, Annabelle Couvert, Éric Dumont

# Cellular concrete waste: an efficient new way for $H_2S$ removal

Morgane POSER[1,3,4], Luis Rodolfo DUARTE E SILVA[1], Pascal PEU[2], Annabelle COUVERT[1], Éric DUMONT[3*]

[1] Univ Rennes, Ecole Nationale Supérieure de Chimie de Rennes, CNRS, ISCR - UMR 6226, F-35000 Rennes, France

[2] INRAE, UR OPAALE, 17 avenue de Cucillé - CS 64427, 35 044 Rennes cedex

[3] Nantes Université, IMT Atlantique, CNRS, GEPEA, UMR 6144, F-44000, Nantes, France

[4] Agence de l'environnement et de la Maîtrise de l'Energie, 20 avenue du Grésillé, BP 90406 49004, Angers Cedex 01, France

*Corresponding author: eric.dumont@imt-atlantique.fr

**Abstract**

The ability of cellular concrete waste (CC) to remove hydrogen sulfide ($H_2S$) from a mimic biogas composed of nitrogen, oxygen and $H_2S$ was investigated using abiotic filtration systems for $H_2S$ concentration up to 1500 mg $m^{-3}$ and Empty Bed Residence Time (EBRT) ranging from 30 to 180 s. The influence of the humidity of the material in $H_2S$ removal was studied. In wetted conditions (relative humidity > 97%), 169 g of $H_2S$ were removed per kg of material. This value is probably lower than the maximum capacity of the cellular concrete since the experiment was ended before the end-of-life of the material. The $H_2S$ elimination capacity of cellular concrete waste could reach up to 32 g $m^{-3}$ $h^{-1}$. These performances are due to complex physico-chemical mechanisms operating simultaneously between $H_2S$ and the different components of cellular concrete (mainly calcium oxide CaO from the calcium silicate hydrate $CaO{\cdot}SiO_2{\cdot}nH_2O$, and ferric oxide $Fe_2O_3$) leading to a modification of the mechanical structure of the material to calcium sulfate (gypsum $CaSO_4{\cdot}2H_2O$) and the production of elemental sulfur (octasulfur $S_8$). Empirical relationships based on $H_2S$ concentration and EBRT were established (i) to predict the Removal Efficiency (RE) of the filtration system (logistic equation); (ii) to assess the operating time of the material. Results obtained suggest that this simple, robust and cheap $H_2S$ removal technology would be a suitable and valuable technique to treat gas flowrates generated by decentralized domestic biogas digesters.

**Keywords:** Hydrogen sulfide; Cellular Concrete Waste; Desulfurization; Separation; Calcium oxide

## Highlights

- $H_2S$ removal from a mimic biogas ($N_2$-$O_2$-$H_2S$) using cellular concrete was investigated
- Cellular concrete is efficient to remove $H_2S$ in abiotic and wetted conditions
- The elimination capacity of the cellular concrete is at least 169 $g_{H_2S}$ per $kg_{material}$
- The elimination capacity of the filtration system reached up to 32 g $m^{-3}$ $h^{-1}$

## 1. Introduction

Biogas, a renewable energy source produced by anaerobic digestion of raw materials such as agricultural and municipal waste, manure, green waste or food waste…, is an alternative to fossil fuels to produce energy. It is a mixture of gaseous compounds, mainly methane ($CH_4$) and carbon dioxide ($CO_2$) but contains also trace amounts of other components such as nitrogen ($N_2$), water vapor ($H_2O$), ammonia ($NH_3$), oxygen ($O_2$) and hydrogen sulfide $H_2S$ [1]. According to the biogas plants and the feedstocks considered, the $H_2S$ gaseous concentrations can reach several thousands of ppm [2]. Hydrogen sulfide is known as a major contaminant in gas since it is both hazardous and corrosive. Its burning leads to the formation of sulfur oxides ($SO_x$) which can affect both the environment and animal health. A $H_2S$ level limited to the range 200-500 ppm is recommended even if a $H_2S$-free biogas is advised [3]. Different technologies exist for $H_2S$ removal, such as biological treatments using microalgae or sulfide oxidizing bacteria and physicochemical treatments (membrane separation, chemical absorption, and physical adsorption techniques including adsorption on activated carbon or iron oxides, and pressure swing adsorption) [1,4–9]. Each of these techniques have their pros and cons in terms of complexity of operation, performance and cost effectiveness. They are suitable for large industrial gas treatment systems, however, they are not well adapted to treat small gas flowrates generated by decentralized domestic biogas digesters such as encountered in India and China for instance [10]. As unpurified biogas burning from small domestic installations used for cooking and lighting leads to significant $SO_x$ emissions, the development of cheap techniques adapted to these decentralized raw gas production systems must be encouraged. A simple

filtration using a bed filled with cellular concrete waste (CC) was recently highlighted to eliminate $H_2S$ from diluted in air under abiotic conditions, i.e. without any microbial population [11,12]. It was suggested that the ability of CC to remove $H_2S$ was due to reactions between $H_2S$ and some components of the material, mainly with calcium carbonate leading to potential gypsum formation [12]. Literature data highlight that $H_2S$ filtration using CC had never been tested to clean raw gas with high $H_2S$ content. The objective of this study was therefore to investigate the ability of a filter bed filled with cellular concrete waste to remove $H_2S$ in a mimic biogas to reach the recommended levels. The influence of the material moisture was investigated. Different operating conditions were applied to determine the filtration performance, in terms of elimination capacity (EC) and removal efficiency (RE). Interactions between $H_2S$ and cellular concrete components, were also studied.

## 2. Materials and methods

The properties and composition of the cellular concrete waste used (Figure 1) were detailed in previous studies dedicated to air cleaning [11,12]. This material, called "copolight", is a mineral material provided by the Florentaise company (France). It is a light (density 547 ± 5 kg $m^{-3}$) and porous (porosity 64%) material, slightly alkaline (pH of surface 9.0 ± 0.1). Its composition in weight is: 50.5% $SiO_2$, 24.6% CaO, 19.7% $SO_3$, 2.2% $Al_2O_3$, 1.4% $P_2O_5$, 1.3% $Fe_2O_3$, 0.2% $K_2O$ [11].

*Figure 1 Cellular concrete waste; scale in centimeters. Left: raw material; Middle: extracted from the top of filter (a) at the end of experiment; Right: extracted from the bottom of filter (a) at the end of experiment*

The experimental set up, depicted in Figure 2, consisted of two identical PVC cylindrical columns (internal diameter 100 mm) filled with the same volume of material (1 m height, V = 7.8 L). For safety reasons, a mimic biogas was used, $CH_4$ being replaced by $N_2$. A nitrogen generator BrezzaNiGen LC–MS (40-1) (purity up to 99.9%) from Gengaz Company (Wasquehal, France) was used to supply $N_2$ continuously into filters (called "Filter (a)" and "Filter (b)"). In spite of the ability of the generator to efficiently purify $N_2$ from air, a weak fraction of oxygen, ranged from 0.5 to 0.8%, was always measured in the nitrogen gas. The $N_2$ flow rate entering a filter was controlled by a mass flowmeter (Model 5850S, Brooks Instruments, Hatfield, USA) and a stream of $H_2S$ (99.7% purity), controlled by another mass flow meter (Model 5850S, Brooks Instruments, Hatfield, USA), was mixed with the $N_2$ flow rate at the bottom of the filter. As a result, the gas flowing through the bed of CC was a mixture of $N_2$-$H_2S$-$O_2$ mimicking an actual raw gas. Thermocouples (K type) were installed on each filter to measure temperatures. To maintain an optimal bed humidity, CC was humidified by a water drop-by-drop system. To respect the operating configuration of an industrial process, the water used was continuously recirculated in each filter. Wet conditions were controlled by humidity sensors (Model EE08, E+E Electronik, Sevres, France) located at the top of filters. $H_2S$ concentrations were measured all along filters by an electrochemical analyzer (Biogas 5000, Geotechnical Instruments Ltd, United Kingdom). Six sampling ports located at 0, 20, 40, 60, 80 and 100 cm from the bottom were used for this purpose. The sampling ports were also used for measuring the pressure drops (pressure sensor Setra, Setra Systems, Inc, Boxborough, USA; 0–700 Pa).

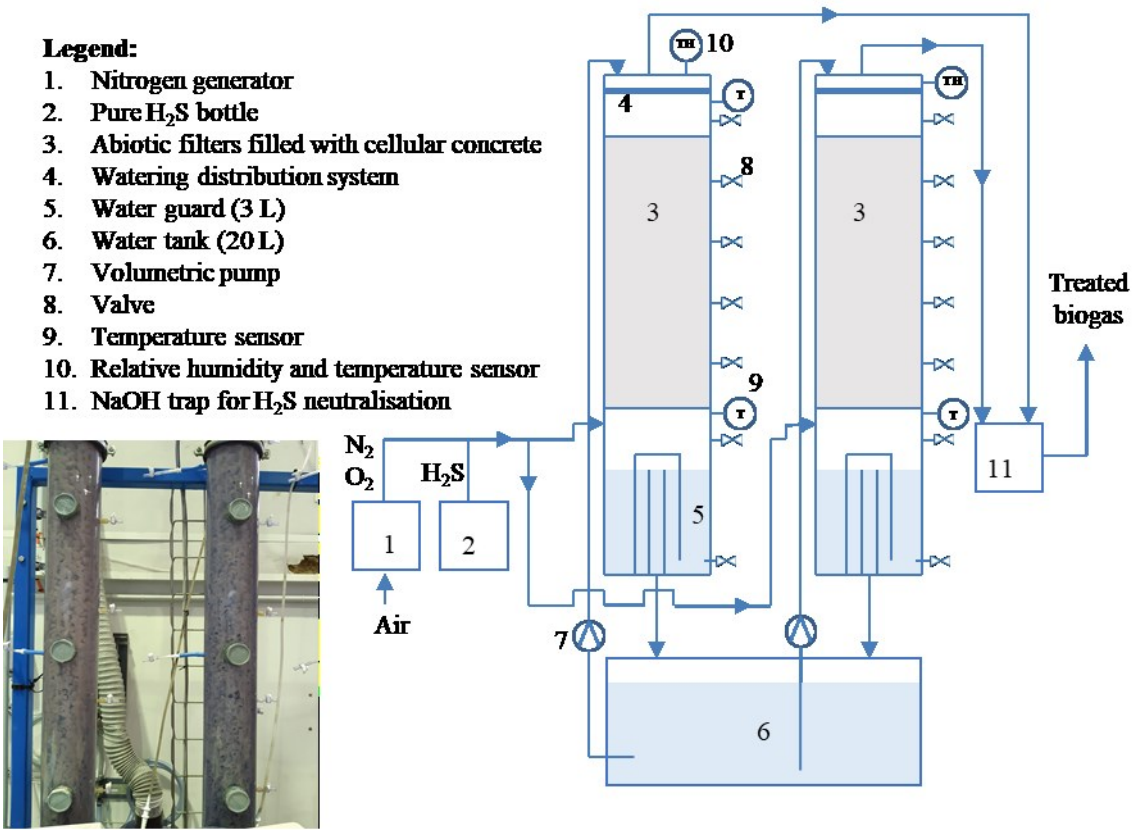


111

112 *Figure 2 Experimental setup (Filter (a): left; Filter (b): right)*

113

114 The parameters used to determine filters performances are reported in Table 1 and the operating
115 conditions are summarized in Table 2. Experiments were performed for two distinct phases.
116 During Phase I (from 97th to 124th day), the influence of the relative humidity on RE was
117 evaluated using Filter (a) at a constant EBRT and $H_2S$ concentration. During Phase II (from
118 146th to 215th day), the influence of EBRT and inlet $H_2S$ concentration on RE were studied for
119 a relative humidity of the gas higher than 93% using the two identical Filters (a) and (b). Before
120 Phase I, to fix the different operation problems encountered, both filters were operated
121 intermittently during a preliminary stage for 96 days. Filters were fed with mimic biogas at day
122 1 and all experimental parameters were continuously recorded from day 43. The $H_2S$
123 concentrations selected (up to 1500 mg $m^{-3}$) were chosen according to the concentrations
124 encountered in a raw biogas. Gas and material temperatures were measured, not controlled. For
125 the running period, temperatures ranged from 17 to 27 °C according to climatic conditions (June
126 to August 2021).

127 The composition of CC samples during $H_2S$ filtration was determined using an energy
128 dispersive X-ray fluorescence (XRF) spectrometer (EDX-800HS, Shimadzu Company) at

different operating times, i.e. at day 1, day 43, day 138 and day 215. X-ray diffraction (XRD) analysis was done to assess the modification in crystalline structure taking place within $H_2S$ filtration (Bruker AXS - D8 advance diffractometer with Cu Kα radiation, λ = 1.5406 Å, step size of 0.02° in 2θ ranged from 5 to 75°, step time of 576 s). Samples of the raw material at the beginning of experiment (day 1) and on the used material at the end of experiment (day 215) were analyzed.

*Table 1* *Parameters used*

| Parameter | Definition | Nomenclature |
|---|---|---|
| Loading Rate LR (g $m^{-3}$ $h^{-1}$) | $\frac{Q}{V} C_{in}$ | $C_{in}$: Inlet gas concentration (g $m^{-3}$) |
| Elimination Capacity EC (g $m^{-3}$ $h^{-1}$) | $\frac{Q}{V} (C_{in} - C_{out})$ | $C_{out}$: Outlet gas concentration (g $m^{-3}$) |
| Empty Bed Residence Time EBRT (s) | $\frac{V}{Q}$ | Q: Gas flow rate ($m^3$ $s^{-1}$) |
| Removal Efficiency RE (%) | $100 \frac{C_{in} - C_{out}}{C_{in}}$ | V: Bed volume of the filter ($m^3$) |

*Table 2* *Operating conditions*

| | Phase | Inlet $H_2S$ concentration $C_{in}$ (mg $m^{-3}$) | EBRT (s) | Loading rate LR (g $m^{-3}$ $h^{-1}$) | Relative humidity RH (%) |
|---|---|---|---|---|---|
| **Filter (a)** | I | 320 | 90 | 12.8 | 15-98 |
| | II(a) | 350 | 90 | 14.0 | >93 |
| | | 500 | | 20.1 | |
| | | 630 | | 25.2 | |
| | | 770 | | 30.3 | |
| | | 910 | | 36.4 | |
| | | 500 | 60 | 30.2 | >93 |
| | | | 45 | 40.2 | |
| | | | 30 | 60.3 | |
| **Filter (b)** | II(b) | 350 | 180 | 7.0 | >93 |
| | | 500 | | 10.0 | |
| | | 900 | | 18.0 | |
| | | 1200 | | 24.0 | |
| | | 1500 | | 29.0 | |
| | | 1500 | 150 | 36.0 | >93 |
| | | | 120 | 45.0 | |
| | | | 100 | 54.0 | |

## 3 Results and discussion

### *3.1 Influence of the relative humidity (RH)*

The influence of the gas relative humidity is displayed at Figure 3(A) (phase I). It can be seen that the higher the relative humidity, the higher the removal efficiency. This finding clearly confirms that wet conditions are required to obtained $H_2S$ removal as evidenced by Lebrun et al. [12] for air treatment. Results from Figure 3(A) demonstrate that relative humidity close to 100% is needed to significantly increase RE. To guarantee the removal efficiency, the humidity of the gas to be treated must be controlled. To some extent, this finding can be compared to results reported in the literature dedicated to the degradation of concrete sewer pipelines in wastewater infrastructure systems [13,14]. From controlled chamber experiments, Joseph et al. [13] investigated the role of relative humidity, temperature and $H_2S$ concentration in air on the concrete degradation. They showed that the influence of the relative humidity was not obvious at low temperature (16-18°C) whereas at higher temperature (25 and 30 °C), its influence was quite clear. This finding was confirmed by Wells and Melchers [14] who studied the corrosion of concrete in 6 different sewers throughout Australia during 48 months. These authors developed a model to predict the corrosion rate. According to this model, the corrosion rate is proportional to (i) the square root of the $H_2S$ concentration in the gas phase, (ii) the temperature via an Arrhenius equation, and (iii) the moisture content of the concrete expressed as the empirical functional relationship depending on the relative humidity (RH) for RH ranged from 85 to 100%:

$$\text{Moisture level} = \frac{0.1602\ \text{RH} - 0.1355}{1 - 0.9770\ \text{RH}} \qquad \text{Equation 1}$$

Applying this empirical relationship to the data reported in Figure 3(A) for RH>85%, the RE vs moisture level is displayed at Figure 3(B). As observed, a clear linear trend between RE and the moisture level exists, even if the regression coefficient is only 0.85. This figure confirms that cellular concrete must be largely wet to achieve a significant removal efficiency. $H_2S$ is then probably first transferred from the gas phase to the aqueous phase to react with CC components.

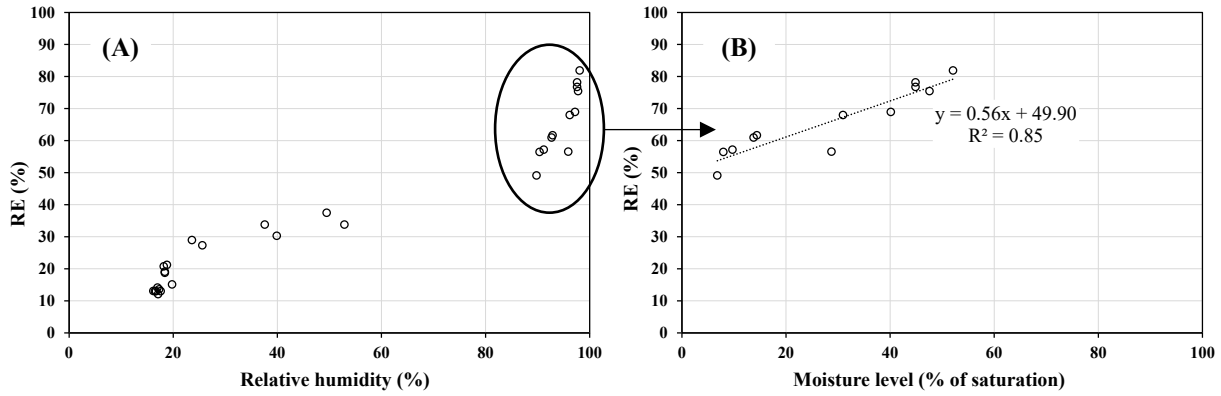


168

169 *Figure 3 Influence of the relative humidity of the gas on $H_2S$ removal efficiency. EBRT = 90 s.*
170 *$H_2S$ inlet concentration = 320 mg $m^{-3}$. (A): RE vs relative humidity of the gas (RH). (B): RE*
171 *vs moisture level of the material calculated from the empirical relationship proposed by [14]:*
172 *moisture level = (0.1602 RH - 0.1355)/(1 - 0.9770 RH) for RH ranged between 85 and 100%*

173

174 ### *3.2 Influence of EBRT and $H_2S$ inlet concentration*

175 The influence of both EBRT and $H_2S$ concentration on RE, recorded for the two identical filters,
176 is given in Figure 4. For a high EBRT (90 s and 180 s for phases II(a) and II(b), respectively),
177 high RE values can be achieved for the overall range of $H_2S$ concentrations applied. RE close
178 to 100% were even recorded for $H_2S$ concentration of 910 mg $m^{-3}$ at EBRT 90 s (phase II(a)).
179 These very high results were obtained during a period of high outdoor temperatures (near to 27
180 °C), well above the values measured in the experiments (from 17 to 20 °C). The temperature of
181 the filtering material must have a large influence on RE. This finding is supported by Wells and
182 Melchers [14] who studied the influence of the temperature of the sewers atmosphere on the
183 corrosion of concrete pipes due to $H_2S$ presence, as indicated above. The contact time between
184 the gas and the material has to be sufficiently long to allow the reaction to take place. In fact,
185 for a given $H_2S$ concentration to be treated (500 and 1500 mg $m^{-3}$ for phases II(a) and II(b),
186 respectively), the decrease of EBRT led to a decrease of performances. Since wet conditions
187 are required for high efficiency, the mass transfer of $H_2S$ between the gas phase and the liquid
188 phase surrounding the material is likely to be limited, especially for a short EBRT. This issue
189 is similar to the one reported in the current literature dedicated to $H_2S$ removal by biofiltration
190 [15], since $H_2S$ has to be dissolved in the aqueous phase to be degraded by microorganisms
191 suspended in the liquid or attached at the surface of the material. To consider the influence of
192 both EBRT and $H_2S$ concentration, all results are gathered in Figure 5 introducing the
193 elimination capacity of filters according to the loading rate to be treated (Table 1). As observed,
194 RE ranged from 70 to 100% for LR (loading rate) up to 30 g $m^{-3}$ $h^{-1}$. This finding is in the same

order of magnitude that those reported in the recent literature dedicated to the anoxic removal of $H_2S$ using conventional biotrickling filters, as reviewed by Valdebenito-Rolak et al. [16]. Compared to anoxic biotrickling filtration, the main advantage to proceed a simple $H_2S$ filtration using CC lies in the fact that micro-organisms and chemical addition of nitrate as electron acceptor are not needed. This technology should be surely more robust, economical and therefore more reliable over the long term than conventional biofiltration at equal performance. In the future, $H_2S$ removal using CC could probably be an interesting alternative to biofiltration depending on the industrial application. Note that the present results obtained for a mimic biogas are better than results found for air treatment since a maximum elimination capacity of 7.8 g $m^{-3}$ $h^{-1}$ was calculated by Lebrun et al. [12], without controlling the humidity of the material. For LR higher than 30 g $m^{-3}$ $h^{-1}$, a decay of performance is observed (Figure 5). Experimental results are significantly scattered, probably partly due to temperature variations mentioned above. As a first approach, the decrease in EC (elimination capacity) for high LR (Figure 5) seems similar to an inhibition curve sometimes observed in $H_2S$ biofiltration although the filter bed was not inoculated. Filters can be naturally colonized by microorganisms, but the role of this potential biomass on $H_2S$ removal should be limited. Moreover, all attempts to model the experimental results from procedures developed for biofilter analysis failed [17,18]. Another modelling approach mainly based on both parameters $H_2S$ concentration and EBRT must be favored.

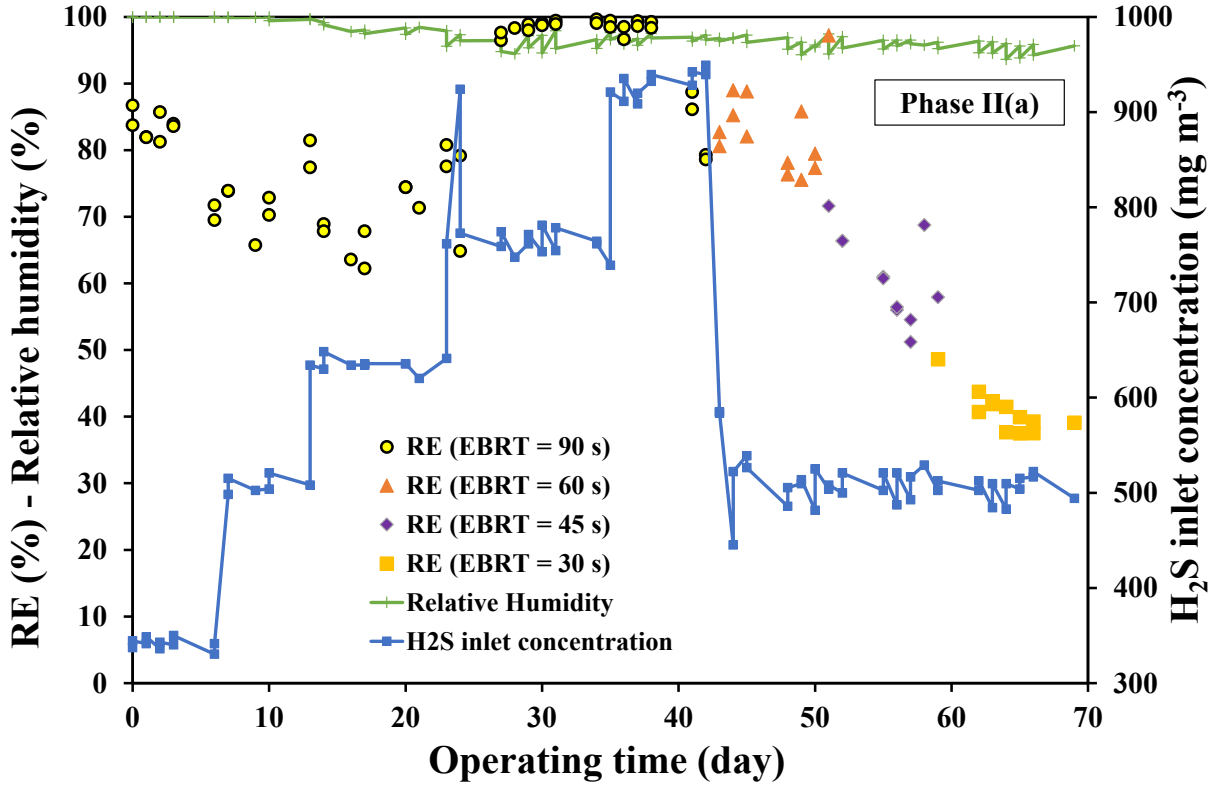


214

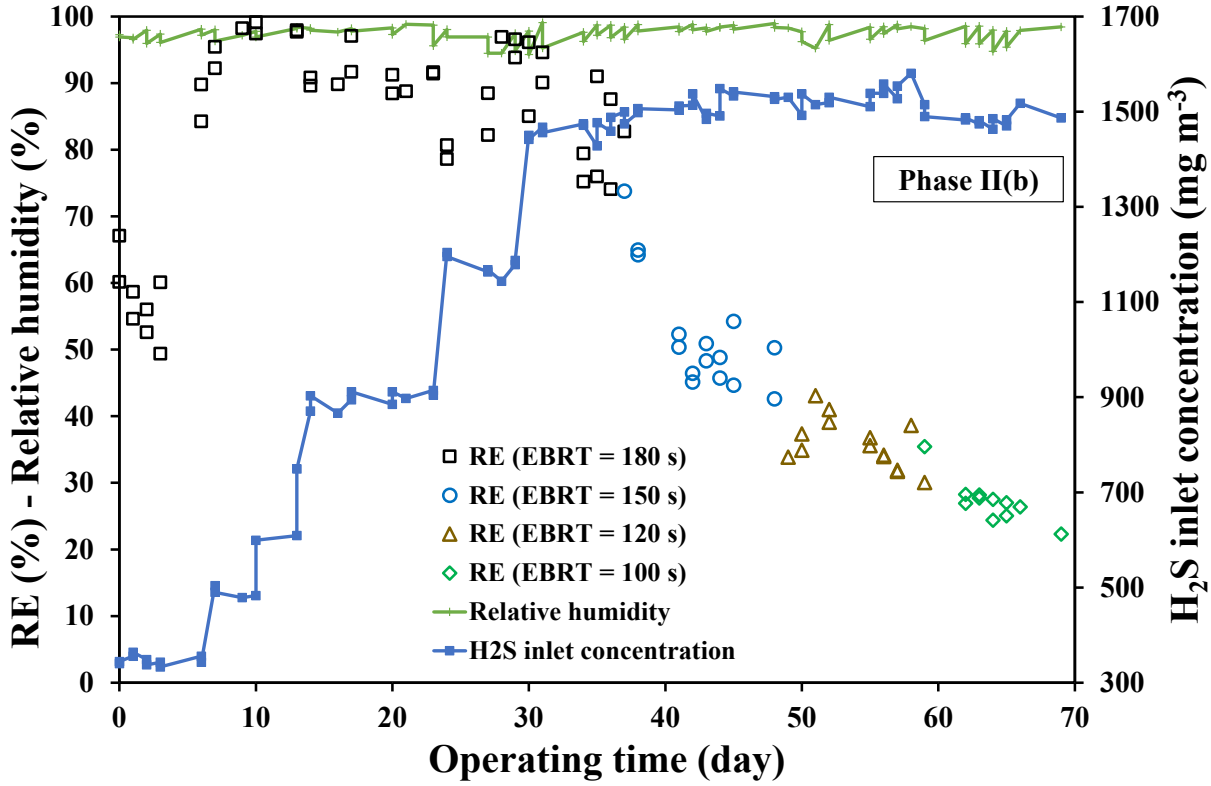


215

216 *Figure 4 Influence of EBRT and $H_2S$ concentration on RE (Phase II(a) and II(b) correspond to*
217 *results recorded using Filter (a) and Filter (b), respectively)*

218

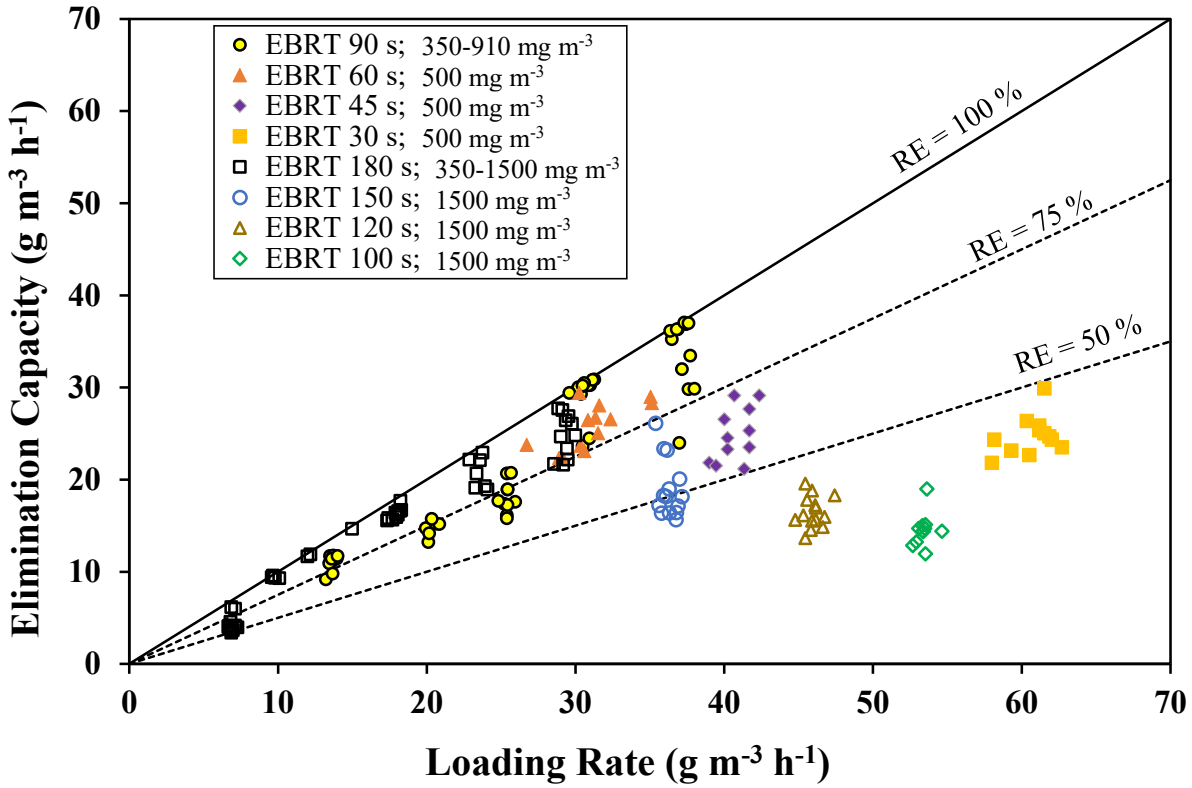


219

220 *Figure 5 EC vs LR for Phases II(a) and II(b) (II(a) closed symbols; II(b) open symbols)*

221

222 ***3.3 Modeling removal efficiency***

223 $H_2S$ concentration profiles along the filters length (H) are given in Figure 6 for two inlet
224 concentrations (500 and 1500 mg $m^{-3}$, respectively) and for different EBRT. Analysis of these
225 profiles can give information about the kinetic regime operating in filter. The decrease in the
226 $H_2S$ concentration along the height of the filter can be well fitted using quadratic forms, but
227 functions are concave down (the second derivatives of these functions being negative) whereas
228 the contrary is usually observed (concave up). All results are gathered in Figure 7 as RE = (1-
229 $C/C_{in}$) versus (H/U). H/U is the time taken for the gas to reach the height H in the filter. For
230 each experiment, H/U is then ranged between 0 at the bottom of the filter (H = 0 m) and EBRT
231 at the top (H = 1 m). For both ranges of $H_2S$ concentration applied, RE clearly depends on the
232 time spent by the gas in the filter. For instance, for a $H_2S$ concentration of 500 mg $m^{-3}$, RE is
233 around 40% when the time spent is 30 s, 70% when the time spent is 45 s, and close to 100%
234 when the time spent is 60 s. A similar finding is achieved for a $H_2S$ concentration of 1500 mg
235 $m^{-3}$. Whatever EBRT is applied to a given inlet concentration, all experiment results are well
236 fitted using a logistic function ($RE=1/[1 + \alpha \exp(-\beta (H/U) C_{in}^{\delta})]$) involving three constants $\alpha$,

β, δ determined using Microsoft Excel® solver (the equation of the parity plot between modeled RE and experimental RE values is y = 0.98 x; $R^2$ = 0.98; not shown):

$$RE = \frac{1}{1 + 26.94 \exp\left(-321.60 \left(\frac{H}{U}\right) C_{in}^{-1.3}\right)}$$ Equation 2

From a physical point of view, the logistic function (sigmoid curve) is a suitable equation for the modelling of experimental data. Indeed, for a residence time of the biogas in the filter (H/U) → ∞, RE logically tends to the asymptote 100% (Figure 7). Moreover, the parameter $\beta\ C_{in}^{\delta}$, which affects the steepness of the curve, shows that the curve approaches the asymptote RE = 1 more rapidly while the inlet $H_2S$ concentration is low. The parameter α corresponds to the number of times the value $RE_{(t=0)}$ must be multiplied to reach RE = 1. As observed in Figure 7, modeled logistic curves begin at $RE_{(t=0)}$ = 0.036 (3.6%) whereas RE should be zero. More sophisticated logistic equations can be found to begin at $RE_{(t=0)}$ closed to 0, however, the curves are not affected for RE > 0.036 and the simple form reported in Figure 7 is preferable. This equation will be useful to design industrial and applied filters.

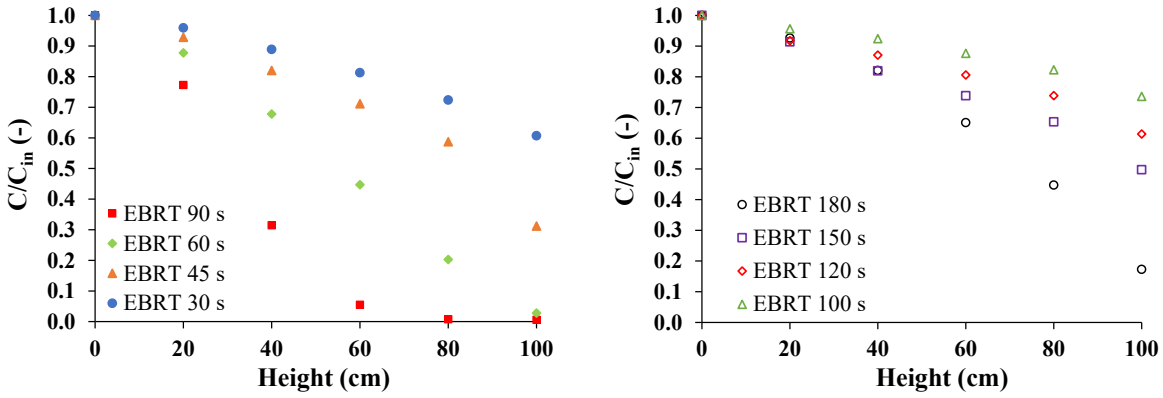


*Figure 6 $H_2S$ concentration profiles according to the length of filters (Left: $C_{in}$ ≈ 500 mg $m^{-3}$: phase II(a); Right: $C_{in}$ ≈ 1500 mg $m^{-3}$: phase II(b))*

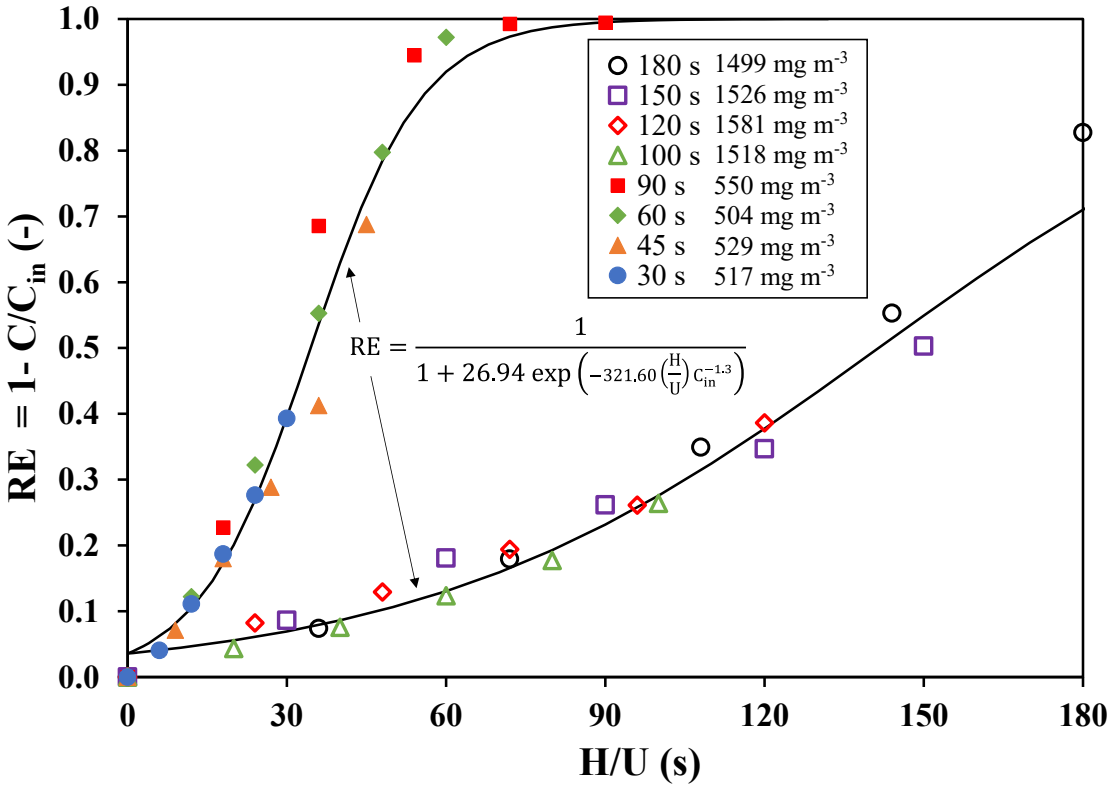


*Figure 7 RE profiles according to the gas residence time in filters (calculated from data reported in Figure 6). Symbols: experimental points; solid curves: logistic equation.*

### *3.4 Possible reactions between $H_2S$ and CC*

The X-ray diffraction (XRD) analysis performed on samples of the raw material at the beginning of experiment and on the used material at the end of experiment is shown in Figure 8. Comparison between spectrograms shows the loss and formation of various components. The raw material was mainly characterized by the presence of tobermorite, chemically represented by $CaO.SiO_2.nH_2O$, and calcite (i.e. calcium carbonate $CaCO_3$). At the end of experiment, both mineral components disappeared while new components appeared, mainly elemental sulfur $S^0$ (under the octasulfur form $S_8$), bassanite ($CaSO_4,0.5H_2O$) and anhydrite ($CaSO_4$), which certainly come from gypsum dehydration ($CaSO_4,2H_2O$) during the drying of samples for analysis. The disappearance of calcium oxides ($CaO.SiO_2.nH_2O$ and $CaCO_3$) and the appearance of calcium sulfate ($CaSO_4,nH_2O$) are consistent with the degradation mechanisms of concrete sewer pipelines due to $H_2S$ formation in wastewater infrastructure systems [19]. The formation of calcium sulfate (gypsum) is due to chemical reactions between the main calcium components of CC with $H_2S$ and sulfuric acid $H_2SO_4$ (Figure 9). Possible reactions with $H_2S$ are:

$CaO + H_2S \rightarrow CaS + H_2O$ Equation 3

$CaO + H_2O \rightarrow Ca(OH)_2$ Equation 4

$Ca(OH)_2 + CO_2 \rightarrow CaCO_3 + H_2O$ Equation 5

$CaCO_3 + H_2S \rightarrow CaS + H_2O + CO_2$ Equation 6

$CaS + 2CO_2 + 2H_2O \rightarrow CaSO_4{,}2H_2O + 2C$ Equation 7

Possible reactions with $H_2SO_4$ are:

$CaCO_3 + H_2SO_4 + H_2O \rightarrow CaSO_4.2H_2O + CO_2$ Equation 8

$Ca(OH)_2 + H_2SO_4 \rightarrow CaSO_4.2H_2O$ Equation 9

$3CaO.2SiO_2.nH_2O + 3H_2SO_4 \rightarrow 3CaSO_4.\ 2H_2O + 2\ SiO_2 + mH_2O$ Equation 10

The presence of sulfuric acid was confirmed by the decrease in pH (from 8.0 to 1.7) of the liquid contained in the water tank and used to humidify the filters. The formation of $H_2SO_4$ can be due to reaction between the sulfur trioxide ($SO_3$) contained in the CC and water, and to the direct oxidation of $H_2S$ with oxygen contained in the mimic biogas (up to 0.8%). According to the following stoichiometric equations, the first product of the $H_2S$ oxidation is $S^0$, which can be converted into $SO_4^{2-}$ in the case of oxygen excess amounts:

$H_2S + 0.5O_2 \rightarrow S^0 + H_2O$ Equation 11

$H_2S + 2O_2 \rightarrow SO_4^{2-} + 2H^+$ Equation 12

$S^0 + 1.5O_2 + H_2O \rightarrow SO_4^{2-} + 2H^+$ Equation 13

Sulfuric acid can also be formed biologically by sulfur oxidizing bacteria (SOB), but an attempt to extract DNA from the surface of a few pieces of CC taken from the filter at the end of the experiment did not reveal the presence of bacteria.

283

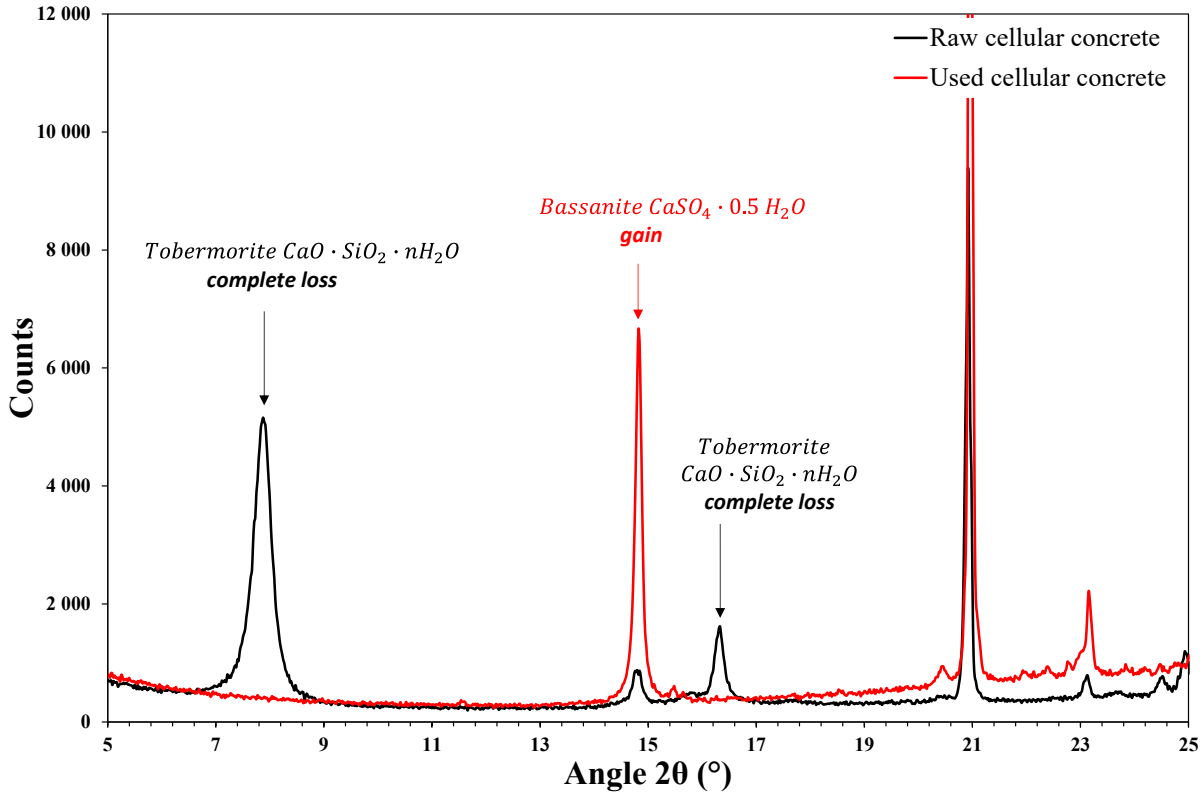


284

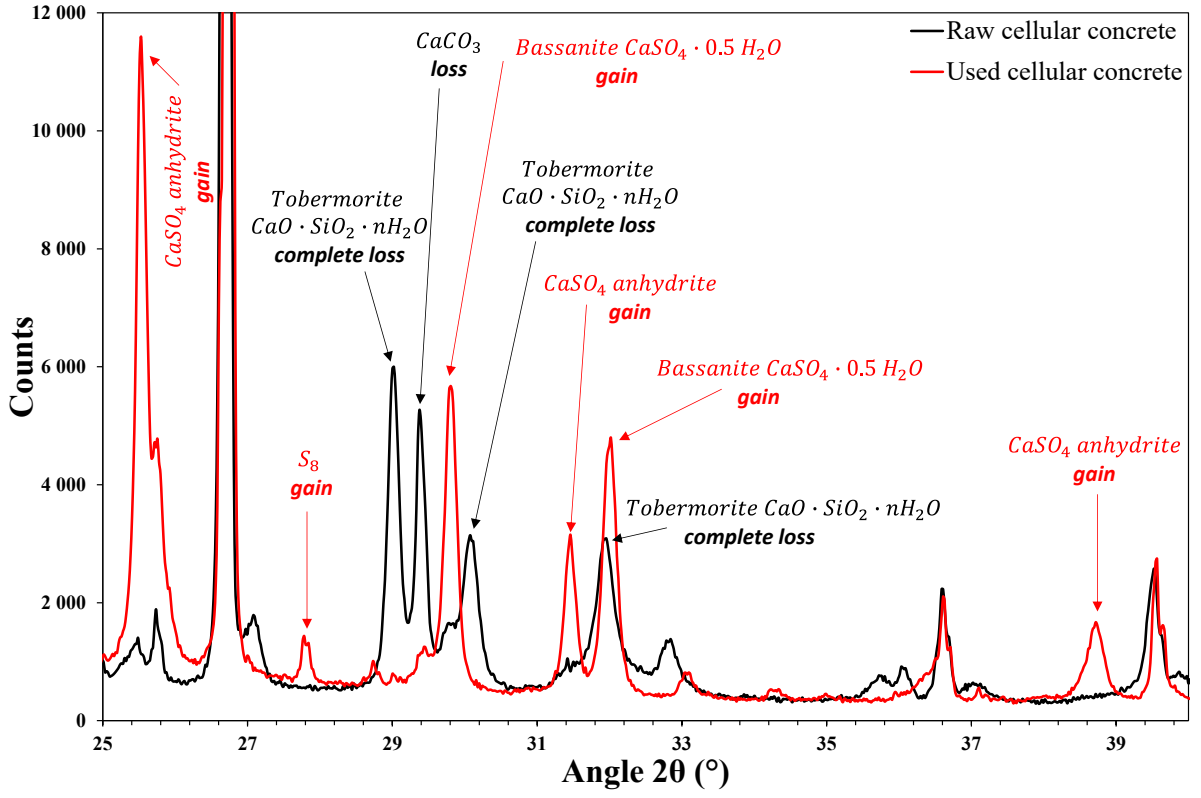


285 *Figure 8 X-ray diffractograms of samples of cellular concrete. Black line: raw material*
286 *(beginning of the experiment); red line: used material (end of the experiment)*

287

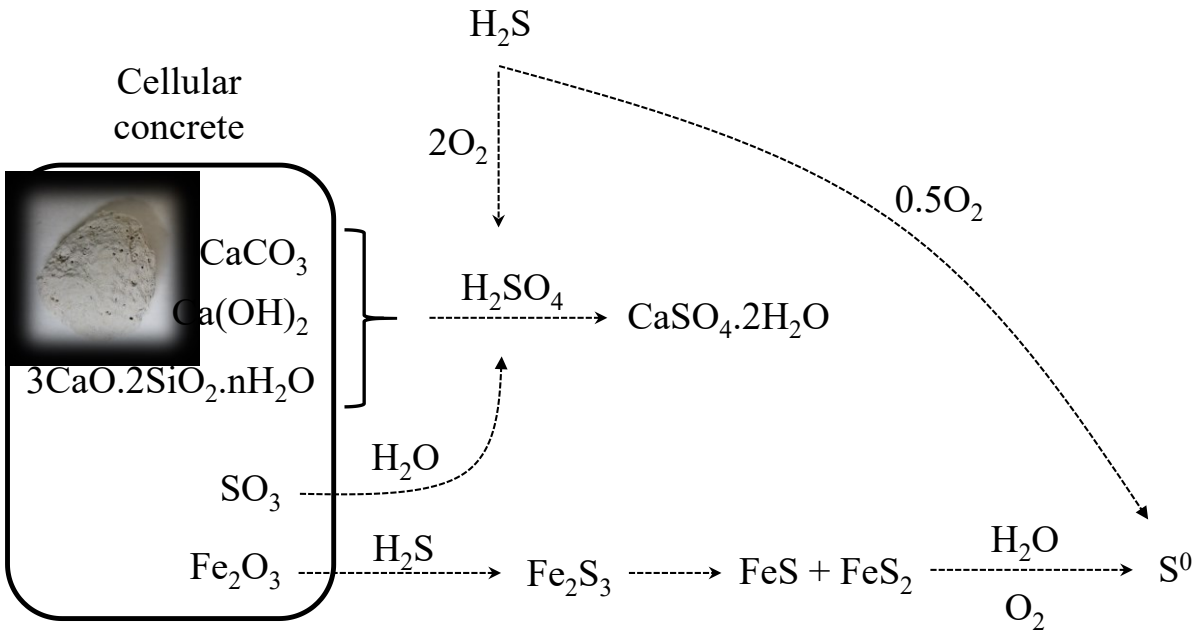


288

289 *Figure 9 Main reactions between the cellular concrete components and $H_2S$ in wet conditions*

290

291 The accumulation of sulfur on CC is clearly evidenced by the increase of the sulfur proportion
292 in the material measured using the energy dispersive X-ray Fluorescence spectrometer (XRF).
293 As Figure 10 shows, the sulfur percentage in the material extracted from Filter (a) increased
294 from 15.4% at day 43 (beginning of continuous measurement records) to 36.2% at day 215,
295 corresponding to an increase of 20.8% in weight. The transformation of the material can also
296 be seen in Figure 1 and Figure 11. The yellow deposit on the surface of the material (Figure 1)
297 clearly reveals the presence of elemental sulfur $S^0$ whereas the origin of the black color at the
298 core has to be identified. This black color is maybe due to the reaction between $H_2S$ and $Fe_2O_3$
299 leading to the formation of iron sulfide (FeS) as will be discussed later. Note that the use of
300 "iron sponges" based on chemical reactions occurring between $Fe_2O_3$ and $H_2S$ is an old
301 technology to remove this component from natural and coal gases. Nonetheless, as observed in
302 Figure 1 and Figure 11, the black color develops from the core to the surface which is
303 counterintuitive since a diffusion-reaction front progresses from the surface to the core. This
304 preliminary observation should be investigated in the future. The reactions between the CC
305 components and the gas also modified the mechanical structure of the material, which became
306 easily friable. As the pieces of material extracted from the filter were highly moist, a simple
307 finger pressure was sufficient to crush them and highlight the dark coloration inside, as
308 observed in Figure 11. Such an operation is not possible using raw cellular concrete waste.

309 In addition to the reaction of $H_2S$ with $O_2$, the production of elemental sulfur can also be due to
310 the presence of oxides into the material itself (Figure 9). The chemistry of $H_2S$ removal at
311 ambient temperature by oxides such as ZnO, CuO, and $Fe_2O_3$ was recently reviewed by
312 Watanabe [9]. According to the composition of cellular concrete waste, $Al_2O_3$ and $Fe_2O_3$ are
313 the main oxides of metals. Cupper, chromium, strontium and zirconium were also detected
314 (Figure 10). Watanabe [9] reported that $H_2S$ reacts with metal oxides to form metal sulfides as:

$$MO_{x(solid)} + xH_2S_{(gas)} \leftrightarrow MS_{x(solid)} + xH_2O_{(gas)} \quad \text{Equation 14}$$

315 This reaction consists of the mechanism described by the following reactions:

$$MO + H_2S \leftrightarrow MS + H_2O \quad \text{Equation 15}$$

$$H_2O + MO \leftrightarrow M(OH)_2 \quad \text{Equation 16}$$

$$M(OH)_2 + H_2S_{(gas)} \leftrightarrow MS + 2H_2O \quad \text{Equation 17}$$

316 Where $MO_x$ is the form of the initial metal oxide and $MS_x$ is the produced metal sulfide after
317 the reaction. Reactivity potential theoretically follows the order $Fe_2O_3 > CuO > ZnO$ [9]. Since
318 the proportion of ferric oxide $Fe_2O_3$ in CC is 1.3% in weight, its presence probably led to the
319 following reactions with $H_2S$, as reported by [20].

$$Fe_2O_3 + 3H_2S \rightarrow Fe_2S_3 + 3H_2O \quad \text{Equation 18}$$

$$Fe_2S_3 \rightarrow FeS + FeS_2 \quad \text{Equation 19}$$

$$FeS_2 \rightarrow FeS + 1/2S_2 \quad \text{Equation 20}$$

320 Subsequently, FeS and $Fe_2S_3$ can react with oxygen leading to the regeneration of ferric oxide:

$$4FeS + 6H_2O + 3O_2 \rightarrow 4Fe(OH)_3 + 1/2S_8 \quad \text{Equation 21}$$

$$2Fe_2S_3 + 6H_2O + 3O_2 \rightarrow 4Fe(OH)_3 + 3/4S_8 \quad \text{Equation 22}$$

$$2Fe_2S_3 + 3O_2 \rightarrow 2Fe_2O_3 + 3/4S_8 \quad \text{Equation 23}$$

321 The overall stoichiometry is:

$$2H_2S + O_2 \rightarrow 1/4S_8 + 2H_2O \quad \text{Equation 24}$$

322 Because disulfur $S_2$ and octasulfur $S_8$ are allotrope forms of elemental sulfur (octasulfur being
323 its main component) the continuous regeneration of $Fe_2O_3$ is probably one of the mechanisms

involved in $H_2S$ removal by cellular concrete waste (Figure 9). Although the mechanisms of the reactions occurring between $H_2S$ and the CC components are partly revealed, the macroscopic analysis from XRD and XRF confirmed the ability of the cellular concrete to react with $H_2S$ and clean the gas.

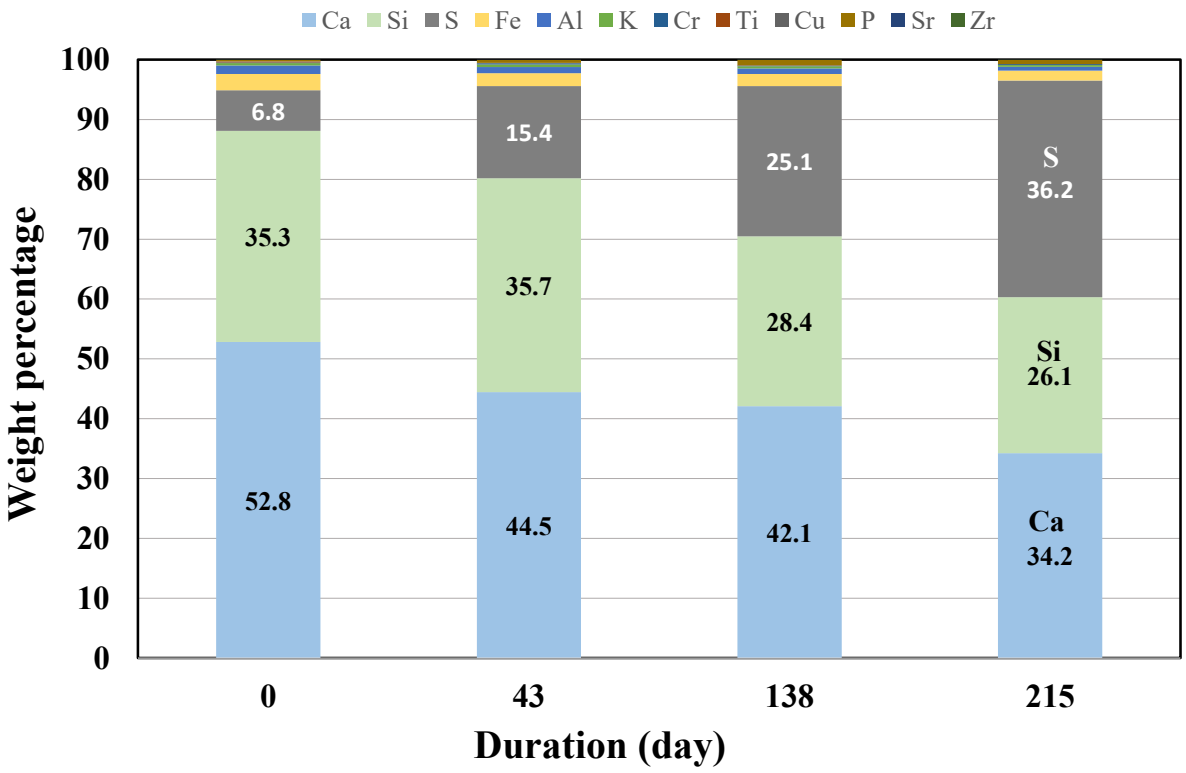


*Figure 10 Modification in composition of the cellular concrete over time extracted from Filter (a)*

*Figure 11 Cellular concrete waste extracted from Filter (a) at the end of experiment. Left: top of filter. Right: bottom of filter*

### *3.5 $H_2S$ elimination capacity*

The cumulative amounts of $H_2S$ removed by both filters are displayed in Figure 12 for the different experimental phases including the preliminary stage. Between day 43 and day 215 (end of experiment), Filter (a) removed 422 $g_{H2S}$ meaning that over the period, 60% of the $H_2S$ entering the filter were removed from biogas. For Filter (b), results are lower, 262 $g_{H2S}$ and 45% of the $H_2S$ entering the filter. This result is due to the fact that the EBRT applied during Phase II (Table 2) were shorter than the calculated residence time needed for high RE in relation with the high $H_2S$ concentration (1500 mg $m^{-3}$; Figure 7). The ability of the CC to react with $H_2S$ is by and large remarkable since 169 g of $H_2S$ were removed per kg of material for Filter (a) at the end of the experiment (105 g per kg for Filter (b); Figure 12). This result is equivalent or higher than data reported in the literature [1,9,21–24] even compared with activated carbons considered as references for $H_2S$ removal (Table 3). Galera Martínez et al. [22] reported, for example, that the capacity of fixed-bed or fluidized-bed reactors using carbon-based materials for $H_2S$ abatement is below 70 g of $H_2S$ per kg of material. These authors studied the ability of two solid wastes containing mainly calcium carbonate to remove $H_2S$ from air at low concentration (280 mg $m^{-3}$) in a triphasic gas-solid-liquid reactor. They reported a removal of 75 g of $H_2S$ per kg of material. The ability of CC to remove $H_2S$ in this study is more than twice as high as those reported in the literature dealing with the reuse of solid waste.

As a first approach, assuming that all $H_2S$ removed has reacted with the CC components to form mainly gypsum and elemental sulfur, the increase of the proportion of sulfur (%S) in the CC over time can be assessed by Equation 25 (Appendix A):

$$\%\,S_{(t)} = \%\,S_{(t=0)} + 100\frac{EC}{\rho_{filter}}\frac{M_S}{M_{H2S}}\,t \qquad \text{Equation 25}$$

With EC the elimination capacity (expressed in kg $m^{-3}$ $h^{-1}$), $\rho_{filter}$ the CC bed density (kg $m^{-3}$), $M_S$ and $M_{H2S}$, the sulfur and hydrogen sulfide molar mass (kg $mol^{-1}$), and t the operating time (h). From data reported in Figure 12, because the average EC value calculated for Filter (a) over the period day 43 to day 215 was 10.4 g $m^{-3}$ $h^{-1}$, the increase in sulfur percentage calculated from Equation 25 should be around 15.9% (with $\rho_{filter}$ calculated from the mass of cellular concrete introduced in the filter bed at the beginning of the experiment). The increase in sulfur proportion determined from XRF measurement (Figure 10) is 20.8% during the same period,

i.e. slightly higher that value determined from Equation 25. Assuming that the pieces of material extracted from the filter (top and bottom) for subsequent analysis are representative of all pieces of material filling the filter, the difference between the two results is probably due to the variation of the $\rho_{filter}$ over time. Because the progressive accumulation of sulfur in the material led indubitably to a modification in its mass and its structure, the density of the filter bed varied over time. Although Equation 25 gives only an order of magnitude of the increase in the sulfur content in the material over time, the formula does give a valuable indication of the ability of CC to remove $H_2S$. At day 215, the sulfur and the calcium contents in Filter (a) were in the same proportion (Figure 10), the cellular concrete was possibly close to its end-of-life.

*Table 3 Summary of main adsorbents used for $H_2S$ removal (25 °C and atmospheric pressure; adapted from [1])*

| **Adsorbents for $H_2S$ removal** | **$H_2S$ elimination capacity (g $kg^{-1}$)** |
|---|---|
| Iron oxide-based (Regenerative, commercial) | 12.7 to 200 |
| Activated carbons (non-Regenerative, commercial) | 1.17 to 211.3 |
| Functionalized adsorbents (non-Regenerative, lab-based) | 1.7 to 496.6 |
| Zeolites (non-Regenerative, commercial) | 0.5 to 53 |
| Metal organic frameworks (non-Regenerative, lab-based) | 13.6 to 618 |

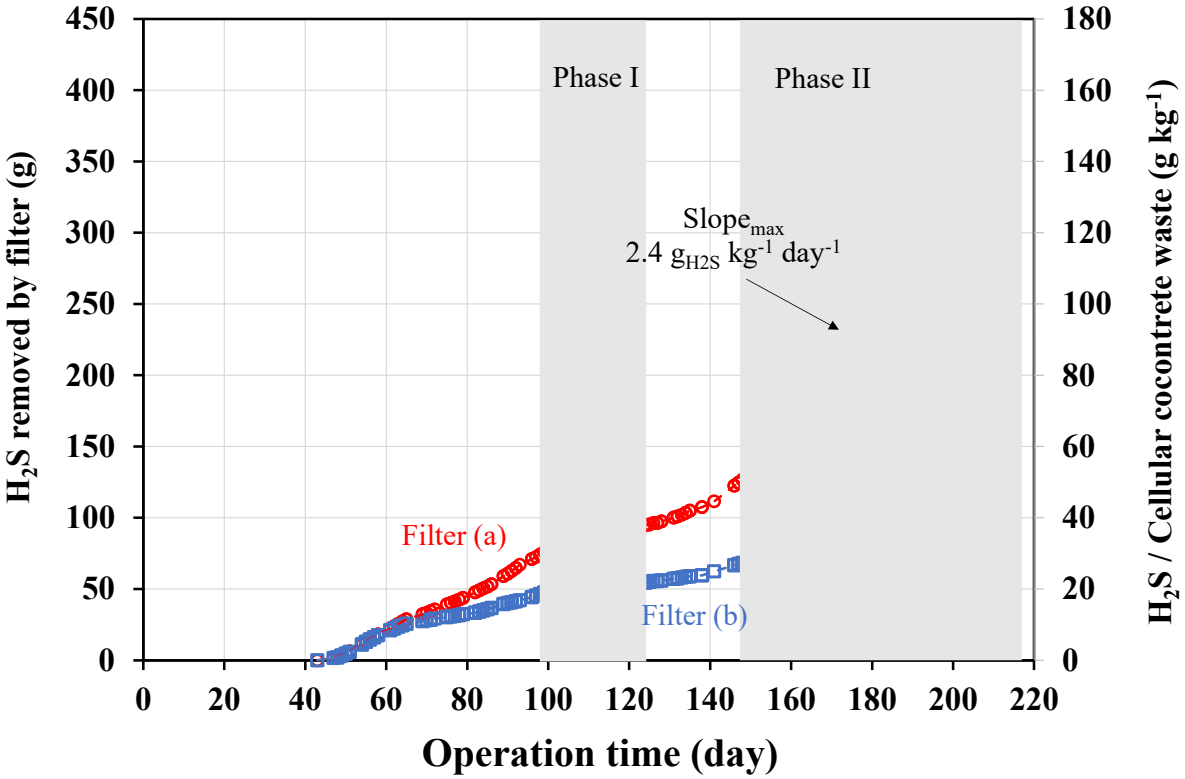


377

378 *Figure 12 Amounts of $H_2S$ removed by both filters over time (the operating conditions are*
379 *summarized in Table 2)*

380

381 ***3.6 Lifetime assessment of cellular concrete***

382 On the basis that reactions between $H_2S$ and calcium oxides lead to gypsum formation
383 (Equation 3 to Equation 10), that fundamentally modifies the structure of the material, the
384 lifetime of the cellular concrete can be assessed by considering the percentage of CaO in the
385 raw material. This lifetime (t in h) can then be determined as a first approach using the Equation
386 26 (Appendix B):

$$t = \rho_{filter} \frac{1}{EC} \%CaO \frac{M_{H2S}}{M_{CaO}} \quad \text{Equation 26}$$

387 As the average EC value calculated over the period (day 43 to day 215) is 10.4 g $m^{-3}$ $h^{-1}$, the
388 operating time of a cellular concrete having 24.9% of CaO, is around 4650 h, i.e. 194 days. This
389 time is by and large consistent with the time life of the material observed during the experiment
390 since the measured performance declined progressively after the end of experiment. Given that
391 t is inversely proportional to EC, the operating time will be shorter as EC increases. According
392 to Figure 12, the maximum amount of $H_2S$ removed was 2.4 $g_{H2S}$ $kg_{CC}^{-1}$ $day^{-1}$ corresponding to

EC = 32 g $m^{-3}$ $h^{-1}$. If these conditions could be continuously maintained, the operating time will be 3 times shorter. Once transformed into gypsum CC waste becomes a new waste, its future must be considered. This new waste could eventually be used as a soil amendment, but it will have to be characterized in terms of toxicity before use. To conclude, as the lifetime of the cellular concrete was calculated for 24.9% of CaO, the result could be improved for higher contents of calcium oxide. Recent work highlighted that synthetic tobermorite ($CaO\ Al_2O_3\ SiO_2\ H_2O$) can be prepared using bio-waste (snail shell) and domestic waste such as soda-lime-silica glass [25]. The synthesis of a functional material especially dedicated to $H_2S$ removal, and made from various waste, would be attractive to imagine. However, the results of the present study have shown that various components of the cellular concrete react with $H_2S$, and synergetic effects probably occurred. The porosity of the material is also a significant parameter that have to be considered [12].

The simple $H_2S$ removal technology based on filtration using cellular concrete waste could be applied at different scales. For large industrial applications, long horizontal filters filled with different crates of cellular concrete would be more appropriate than a very high column. For small decentralized domestic biogas digesters, the size of filters would be small (some liters) and consequently a simple system could be use. Whatever the scale of the application, maintaining the moisture content of the material and changing the material at the end of its life are the two parameters that will dictate the technology and the design of the filters. Concerning the future of the cellular concrete waste having reacted with $H_2S$, the new waste material obtained could be possibly recyclable as a soil amendment as it is mainly composed of gypsum. Nonetheless, it will have to be characterized in terms of toxicity before use. As the findings reported in this study were based on a mimic biogas, future experiments should be performed in real conditions by using a real biogas. The presence of others gases in the biogas, mainly carbon dioxide but also oxygen, could have a significant influence on the empirical relationship predicting the removal efficiency (Equation 2).

## 4 Conclusions

The ability of cellular concrete waste to satisfactorily remove $H_2S$ from a biogas mimic composed of $N_2$-$O_2$-$H_2S$ was evidenced. Many complex physico-chemical mechanisms must occur simultaneously between $H_2S$ and the components of cellular concrete waste (mainly calcium oxides and ferric oxide), leading to a modification of the composition of the material.

During the study, 169 g of $H_2S$ were removed per kg of material at the end of the experiment, it is significantly higher than data reported in the literature. This result is probably lower than the maximum capacity of the CC since the experiment was ended before the end-of-life of the material. The $H_2S$ elimination capacity of the CC was also measured to be up to 32 g $m^{-3}$ $h^{-1}$, which is equal to or better than the performance of biofiltration systems. This simple $H_2S$ removal technology, certainly more robust and economical than conventional biofiltration with the same performance, could take its place in numerous industrial cases. A first empirical relationship, depending of both the $H_2S$ concentration of the biogas and the EBRT applied, was proposed to predict the removal efficiency of a filtration system (logistic equation, Equation 2). An equation was also proposed to predict the lifetime of the material. These findings suggest that $H_2S$ removal using cellular concrete waste could be suitable to treat small gas flowrates generated by decentralized domestic biogas digesters. This pre-experiment based on a mimic biogas must be, in the future, validated in real conditions by using a real biogas.

## Appendix A

Assuming that $H_2S$ reacts with components of CC to mainly form gypsum and elemental sulfur, the increase in sulfur proportion of CC over time can be assessed according to the following way (S = sulfur):

$$\text{Mass } S_{(t)} = \text{Mass } S_{(t=0)} + \text{Mass } S_{(\text{transferred from gas to cellular concrete})} \quad \text{Eq. (A.1)}$$

$$\text{Mass } S_{(t)} = \text{Mass } S_{(t=0)} + Q\,(C_{in} - C_{out})\,\frac{M_S}{M_{H2S}}\,t \quad \text{Eq. (A.2)}$$

With Q the gas flowrate ($m^3$ $h^{-1}$), $C_{in}$ and $C_{out}$ (kg $m^{-3}$) the gas $H_2S$ concentrations at the inlet and outlet of the filter, respectively, t (h) the operating time, $M_S$ and $M_{H2S}$, the of sulfur and hydrogen sulfide molar mass (kg $mol^{-1}$). Dividing by the mass of CC used ($Mass_{CC}$ in kg), the following equation is obtained:

$$\frac{\text{Mass } S_{(t)}}{Mass_{CC}} = \frac{\text{Mass } S_{(t=0)}}{Mass_{CC}} + \frac{Q\,(C_{in} - C_{out})}{Mass_{CC}}\,\frac{M_S}{M_{H2S}}\,t \quad \text{Eq. (A.3)}$$

As the mass of cellular concrete in the filter is ($Mass_{CC} = V\ \rho_{filter}$) with V ($m^3$) the volume of the filter bed and $\rho_{filter}$ (kg $m^{-3}$) the CC bed density, Eq. (A.3) gives:

$$\text{Fraction } S_{(t)} = \text{Fraction } S_{(t=0)} + \frac{Q\,(C_{in} - C_{out})}{V\,\rho_{filter}}\,\frac{M_S}{M_{H2S}}\,t \qquad \text{Eq. (A.4)}$$

According to the definition of the elimination capacity (EC) given in Table 1, and multiplying each term by 100, the increase in sulfur proportion over time is given according to the following relation:

$$\%\,S_{(t)} = \%\,S_{(t=0)} + 100\frac{EC}{\rho_{filter}}\,\frac{M_S}{M_{H2S}}\,t \qquad \text{Eq. (A.5)}$$

## Appendix B

The lifetime (t in h) of the cellular concrete can be assessed by considering the percentage of CaO in the raw material:

$$t = \frac{\text{Mass of } H_2S \text{ reacting with CaO}}{\text{Mass flow of } H_2S \text{ removed from the gas}} \qquad \text{Eq. (B.1)}$$

$$t = \frac{\%CaO\;\;Mass_{CC}\;\;\frac{M_{H2S}}{M_{CaO}}}{Q\,(C_{in} - C_{out})} \qquad \text{Eq. (B.2)}$$

With parameters given in Appendix A and $M_{CaO}$, the molar mass (kg mol$^{-1}$) of calcium oxide. As previously detailed, the mass of cellular concrete $Mass_{CC} = (V\,\rho_{filter})$ and:

$$t = \rho_{filter}\,\frac{V}{Q\,(C_{in} - C_{out})}\;\;\%CaO\;\;\frac{M_{H2S}}{M_{CaO}} \qquad \text{Eq. (B.3)}$$

This equation can be rewritten under the following forms, either by introducing the Elimination Capacity or the Removal Efficiency and the Empty Bed Residence Time given in Table 1 using the appropriate units (EC in kg m$^{-3}$ h$^{-1}$ and EBRT in h):

$$t = \rho_{filter}\,\frac{1}{EC}\;\;\%CaO\;\;\frac{M_{H2S}}{M_{CaO}} \qquad \text{Eq. (B.4)}$$

$$t = \rho_{filter}\,\frac{V}{Q\;\;C_{in}\,RE}\;\;\%CaO\;\;\frac{M_{H2S}}{M_{CaO}} \qquad \text{Eq. (B.5)}$$

$$t = \rho_{filter}\,\frac{EBRT}{C_{in}\,RE}\;\;\%CaO\;\;\frac{M_{H2S}}{M_{CaO}} \qquad \text{Eq. (B.6)}$$

**Acknowledgements**

The authors would like to thank ADEME (N° TEZ19-041) and the Region of Brittany (N°1169) for their financial support.

**Conflict of interest**

The authors declare no conflict of interest.

**Acknowledgments**: To the Département Systèmes Energétiques et Environnement of IMT Atlantique (Nantes, France). Also special thank to Yvan Gouriou for his continuous support in process management and Denys Grekov for the XRD analysis.

**CRediT author statement**

**Morgane POSER**: methodology, resources, validation, formal analysis, investigation, data curation, writing—original draft preparation, writing—review and editing **Luis Rodolfo DUARTE E SILVA**: resources, formal analysis, investigation, data curation **Pascal PEU**: validation, writing—review and editing, supervision **Annabelle COUVERT**: Conceptualization, validation, writing—review and editing, supervision, project administration, funding acquisition **Éric DUMONT**: Conceptualization, methodology, validation, writing—original draft preparation, writing—review and editing, supervision

**References**

[1] A. Golmakani, S. Ali Nabavi, B. Wadi, V. Manovic, Advances, challenges, and perspectives of biogas cleaning, upgrading, and utilisation, Fuel. 317 (2022) 123085. https://doi.org/10.1016/j.fuel.2021.123085.

[2] P. Peu, J.-F. Sassi, R. Girault, S. Picard, P. Saint-Cast, F. Béline, P. Dabert, Sulphur fate and anaerobic biodegradation potential during co-digestion of seaweed biomass (Ulva sp.) with pig slurry, Bioresour. Technol. 102 (2011) 10794–10802. https://doi.org/10.1016/j.biortech.2011.08.096.

[3] B. Khoshnevisan, P. Tsapekos, N. Alfaro, I. Díaz, M. Fdz-Polanco, S. Rafiee, I. Angelidaki, A review on prospects and challenges of biological H2S removal from

biogas with focus on biotrickling filtration and microaerobic desulfurization, Biofuel Res. J. 4 (2017) 741–750. https://doi.org/10.18331/BRJ2017.4.4.6.
[4] N. Abatzoglou, S. Boivin, A review of biogas purification processes, Biofuels Bioprod. Biorefining. 3 (2009) 42–71. https://doi.org/10.1002/bbb.117.
[5] D. Andriani, A. Rajani, Kusnadi, A. Santosa, A. Saepudin, A. Wresta, T.D. Atmaja, A review on biogas purification through hydrogen sulphide removal, IOP Conf. Ser. Earth Environ. Sci. 483 (2020) 012034. https://doi.org/10.1088/1755-1315/483/1/012034.
[6] E. Dumont, H2S removal from biogas using bioreactors: a review, Int. J. Energy Environ. (2015) 479–498.
[7] A. Ghimire, R. Gyawali, P.N.L. Lens, S.P. Lohani, Technologies for removal of hydrogen sulfide (H2S) from biogas, in: Emerg. Technol. Biol. Syst. Biogas Upgrad., Elsevier, 2021: pp. 295–320. https://doi.org/10.1016/B978-0-12-822808-1.00011-8.
[8] G. Piechota, Multi-step biogas quality improving by adsorptive packed column system as application to biomethane upgrading, J. Environ. Chem. Eng. 9 (2021) 105944. https://doi.org/10.1016/j.jece.2021.105944.
[9] S. Watanabe, Chemistry of H2S over the surface of Common solid sorbents in industrial natural gas desulfurization, Catal. Today. 371 (2021) 204–220. https://doi.org/10.1016/j.cattod.2020.05.064.
[10] G. Piechota, B. Igliński, Biomethane in Poland—Current Status, Potential, Perspective and Development, Energies. 14 (2021) 1517. https://doi.org/10.3390/en14061517.
[11] M. Ben Jaber, A. Couvert, A. Amrane, P. Le Cloirec, E. Dumont, Removal of hydrogen sulfide in air using cellular concrete waste: Biotic and abiotic filtrations, Chem. Eng. J. 319 (2017) 268–278. https://doi.org/10.1016/j.cej.2017.03.014.
[12] G. Lebrun, A. Couvert, É. Dumont, H2S removal using cellular concrete waste as filtering material: Reactions identification and performance assessment, J. Environ. Chem. Eng. 7 (2019) 102967. https://doi.org/10.1016/j.jece.2019.102967.
[13] A.P. Joseph, J. Keller, H. Bustamante, P.L. Bond, Surface neutralization and H2S oxidation at early stages of sewer corrosion: Influence of temperature, relative humidity and H2S concentration, Water Res. 46 (2012) 4235–4245. https://doi.org/10.1016/j.watres.2012.05.011.
[14] T. Wells, R.E. Melchers, Modelling concrete deterioration in sewers using theory and field observations, Cem. Concr. Res. 77 (2015) 82–96. https://doi.org/10.1016/j.cemconres.2015.07.003.
[15] H. Huynh Nhut, V. Le Thi Thanh, L. Tran Le, Removal of H2S in biogas using biotrickling filter: Recent development, Process Saf. Environ. Prot. 144 (2020) 297–309. https://doi.org/10.1016/j.psep.2020.07.011.
[16] E. Valdebenito-Rolack, R. Díaz, F. Marín, D. Gómez, F. Hansen, Markers for the Comparison of the Performances of Anoxic Biotrickling Filters in Biogas Desulphurisation: A Critical Review, Processes. 9 (2021) 567. https://doi.org/10.3390/pr9030567.
[17] M. Ben Jaber, A. Couvert, A. Amrane, F. Rouxel, P. Le Cloirec, E. Dumont, Biofiltration of H2S in air—Experimental comparisons of original packing materials and modeling, Biochem. Eng. J. 112 (2016) 153–160. https://doi.org/10.1016/j.bej.2016.04.020.
[18] É. Dumont, Validation of a rapid procedure to determine biofilter performances, J. Environ. Chem. Eng. 5 (2017) 2668–2680. https://doi.org/10.1016/j.jece.2017.05.022.
[19] H. Yuan, P. Dangla, P. Chatellier, T. Chaussadent, Degradation modelling of concrete submitted to sulfuric acid attack, Cem. Concr. Res. 53 (2013) 267–277. https://doi.org/10.1016/j.cemconres.2013.08.002.

[20] A. Davydov, K.T. Chuang, A.R. Sanger, Mechanism of H2S Oxidation by Ferric Oxide and Hydroxide Surfaces, J. Phys. Chem. B. 102 (1998) 4745–4752. https://doi.org/10.1021/jp980361p.
[21] S. Asaoka, H. Okamura, R. Morisawa, H. Murakami, K. Fukushi, T. Okajima, M. Katayama, Y. Inada, C. Yogi, T. Ohta, Removal of hydrogen sulfide using carbonated steel slag, Chem. Eng. J. 228 (2013) 843–849. https://doi.org/10.1016/j.cej.2013.05.065.
[22] M. Galera Martínez, D. Pham Minh, A. Nzihou, P. Sharrock, Valorization of calcium carbonate-based solid wastes for the treatment of hydrogen sulfide in a semi-continuous reactor, Chem. Eng. J. 360 (2019) 1167–1176. https://doi.org/10.1016/j.cej.2018.10.169.
[23] S. Lee, D. Kim, Enhanced adsorptive removal of hydrogen sulfide from gas stream with zinc-iron hydroxide at room temperature, Chem. Eng. J. 363 (2019) 43–48. https://doi.org/10.1016/j.cej.2019.01.122.
[24] E. Mulu, M.M. M'Arimi, R.C. Ramkat, A review of recent developments in application of low cost natural materials in purification and upgrade of biogas, Renew. Sustain. Energy Rev. 145 (2021) 111081. https://doi.org/10.1016/j.rser.2021.111081.
[25] Y.D. Lamidi, S.S. Owoeye, S.M. Abegunde, Preparation and characterization of synthetic tobermorite (CaO–Al2O3–SiO2–H2O) using bio and municipal solid wastes as precursors by solid state reaction, Bol. Soc. Esp. Cerámica Vidr. 61 (2022) 76–81. https://doi.org/10.1016/j.bsecv.2020.07.003.